Neuroscience Research 218 (2025) 104922

Contents lists available at ScienceDirect

Neuroscience Research

journal homepage: www.sciencedirect.com/journal/neuroscience-research

Alteration of perineuronal nets and parvalbumin interneurons in prefrontal cortex and hippocampus, and correlation with blood corticosterone in activity-based anorexia model mice

Hoang Duy Nguyen [a], Haruko Miyazaki [b], Hiroki Kawai [c], Ziyi Wang [b], Shinji Sakamoto [d], Manabu Takaki [d], Toshitaka Oohashi [a,b,*]

[a] Department of Molecular Biology and Biochemistry, Okayama University Graduate School of Medicine, Dentistry and Pharmaceutical Sciences, Okayama, Japan
[b] Department of Molecular Biology and Biochemistry, Okayama University Faculty of Medicine, Dentistry and Pharmaceutical Sciences, Okayama, Japan
[c] Department of Neuropsychiatry, Okayama University Graduate School of Medicine, Dentistry and Pharmaceutical Sciences, Okayama, Japan
[d] Department of Neuropsychiatry, Okayama University Faculty of Medicine, Dentistry and Pharmaceutical Sciences, Okayama, Japan

ARTICLE INFO

Keywords:
anorexia nervosa
activity-based anorexia
perineuronal nets
parvalbumin
corticosterone
prefrontal cortex
hippocampus

ABSTRACT

Anorexia nervosa (AN) is an eating disorder characterized by restricted energy intake, severely underweight status, and frequent hyperactivity. Previous research has shown structural and functional alterations in the medial prefrontal cortex (mPFC) and hippocampus of AN patients. To investigate the pathological mechanism of AN, we analyzed the expression and distribution of parvalbumin (PV) interneurons and perineuronal nets (PNNs), which are implicated in the pathology of neuropsychiatric disorders, in the mPFC and hippocampus dorsal (HPCd) and ventral (HPCv) using an activity-based anorexia (ABA) mouse model. We found that PNN expression and density increased in the mPFC, with minor alterations in the HPCd and HPCv of ABA mice. The expression and distribution of PV neurons were unchanged in the brains of ABA mice, except for a regional decrease in PV-expressing neuron density in the HPCd. Co-localization analysis showed an increased number of PNNs enwrapping PV-negative neurons in the mPFC of ABA mice. Furthermore, the upregulation of PNN expression in the mPFC was positively correlated with elevated blood corticosterone levels, a well-known stress indicator, in ABA mice. Our findings suggest that the increased expression and distribution of PNNs surrounding PV-negative neurons in the mPFC may indicate the pathological mechanisms of AN.

1. Introduction

Anorexia nervosa (AN) is an eating disorder characterized by the restriction of energy intake, leading to significantly low body weight (BW), intense fear of gaining weight, and disturbance in the way in which one's BW or shape is experienced (American Psychiatric Association, 2013). AN mainly affects adolescent females, with the highest incidence at approximately age 15 years and female-to-male ratio as high as 13–14:1 (van Eeden et al., 2021). Abnormally high levels of physical activity can be observed in up to 80 % of AN patients (Melissa et al., 2020), indicating that hyperactivity is a major symptom of AN. AN is a severe disease, with a lifetime prevalence of up to 4 % in women and sixfold increased mortality risk (van Eeden et al., 2021). AN treatment lacks strong scientific evidence, with a recovery rate below 50 % (Brockmeyer et al., 2018) and a relapse rate of approximately 25 % (Khalsa et al., 2017). To date, no clear predictive markers for AN development have been identified (Charrat et al., 2023), hindering the development of effective target-based treatments.

Given the high prevalence, high mortality rate, and lack of pharmacological treatments for AN, a deeper understanding of the underlying mechanisms is urgently needed. The activity-based anorexia (ABA) animal model was established in rats by Hall and Hanford in 1953 and was later expanded to other species, including mice (Klenotich and Dulawa, 2012). By providing an animal running wheel and restricting

Abbreviations: PV, parvalbumin; PNNs, perineuronal nets; AN, anorexia nervosa; MPFC, medial prefrontal cortex; HPCd, hippocampus dorsal; HPCv, hippocampus ventral; ABA, activity-based anorexia.

* Correspondence to: Department of Molecular Biology and Biochemistry, Okayama University Graduate School of Medicine, Dentistry and Pharmaceutical Sciences, 2-5-1 Shikata-cho, Kita-ku, Okayama 700-8558, Japan.
E-mail address: oohashi@cc.okayama-u.ac.jp (T. Oohashi).

https://doi.org/10.1016/j.neures.2025.104922
Received 10 April 2025; Received in revised form 23 May 2025; Accepted 13 June 2025
Available online 14 June 2025
0168-0102/© 2025 The Authors. Published by Elsevier B.V. This is an open access article under the CC BY-NC license (http://creativecommons.org/licenses/by-nc/4.0/).

feeding time, they start to display characteristic signs similar to those of patients with AN: a rapid decrease in BW, reduced food intake, and hyperactivity (Schalla and Stengel, 2019). The ABA model has become a valuable tool for AN studies, such as those on the brain and its molecular pathology (Foldi, 2024).

The perineuronal net (PNN) is a type of brain extracellular matrix with a condensed lattice-like structure enwrapping the neuron soma and dendrites (Oohashi et al., 2015; Fawcett et al., 2019). Previous studies have demonstrated that PNNs are involved in many aspects of brain physiology and function, including ion buffering (Morawski et al., 2015), molecular signaling (Beurdeley et al., 2012; Dick et al., 2013), plasticity (de Vivo et al., 2013; Miyata and Kitagawa, 2015), and memory (Romberg et al., 2013; Happel et al., 2014; Carulli et al., 2020). PNNs predominantly enwrap parvalbumin (PV) interneurons (Lupori et al., 2023), the most common subtype of GABAergic interneurons that are critical for maintaining normal excitatory and inhibitory neurotransmission and regulating neural activity (Ferguson and Gao, 2018; Hu et al., 2014; Packer and Yuste, 2011). PNNs not only influence and maintain PV neuron activity (Dityatev et al., 2007; Balmer, 2016; Favuzzi et al., 2017), but also serve as protective barriers against harmful elements such as oxidative stress (Cabungcal et al., 2013; Suttkus et al., 2014). Owing to their functional importance, PNNs and PV neurons have been one of the main areas of interest in the psychiatric research field, with evidence of PV neuron vulnerability and PNN alterations in stress-related disorders in human and animal models (Pantazopoulos and Berretta, 2016; Selten et al., 2018; Wen et al., 2018; Perlman et al., 2021). However, the roles of PNNs and PV neurons in AN and ABA pathologies remain unclear.

The medial prefrontal cortex (mPFC) and hippocampus (HPC) are two brain areas that are highly involved in AN pathology, with evidence showing structural and functional alterations in AN patients (Burkert et al., 2015; Scharner and Stengel, 2019; Keeler et al., 2020; Tose et al., 2024). The mPFC and HPC are involved in stress- and food-related behaviors and are extensively interconnected (Fanselow and Dong, 2010; Sigurdsson and Duvarci, 2015; Fuglset et al., 2016; Le Merre et al., 2021). The HPC is a complex brain area with different anatomical structures and functions between the dorsal hippocampus (HPCd) and ventral hippocampus (HPCv) (Bannerman et al., 2004). However, the HPCd and HPCv can interact via several routes (Fanselow and Dong, 2010), and both are involved in stress modulation (Bittar and Labonté, 2021; Shi et al., 2023). Neuronal mapping studies have demonstrated that both HPCd and HPCv send direct neuronal inputs to the mPFC area (Ährlund-Richter et al., 2019; Qiu et al., 2024). Furthermore, as part of the limbic system, the mPFC and HPC can modulate the hypothalamic-pituitary-adrenocortical (HPA) axis and release of corticosteroid hormones as a stress response (Mora et al., 2012). AN patients showed higher cortisol levels than healthy adolescents (Luz Neto et al., 2019), with evidence of chronic HPA axis activation in many AN patients (Lawson et al., 2009; Misra et al., 2006, 2004). Corticosteroid hormones are known to affect synaptic transmission and plasticity in HPC (Champagne et al., 2008; Gould and Tanapat, 1999) and the PFC (Lamanna et al., 2021; Maroun and Richter-Levin, 2003; Treccani et al., 2014), indicating a possible link between stress hormones and PV neurons as well as PNNs in these brain areas.

Using these findings, we investigated the potential changes in PV neurons and PNNs in the mPFC and HPC of adolescent female mice under the ABA paradigm by quantifying the intensity and number of PV-expressing neurons and PNNs in the mPFC, HPCd, and HPCv areas. We analyzed each area by regions and layers, because the distribution of PV neurons and PNNs in the mouse brain has been reported to be region- and layer-specific (Ueno et al., 2017b; Yamada et al., 2015). The mesh-like structure of PNNs makes traditional segmentation methods difficult; therefore, we utilized artificial intelligence (AI)-assisted PolygonAI software (Slaker et al., 2016) for better consistency and reproducibility of the measurement. We also measured corticosterone levels in ABA and control mice to examine the potential correlations between corticosterone, PV neurons, and PNNs. Our findings reveal region-specific changes in these markers in the ABA brain, providing insights into the neurobiological mechanisms underlying AN pathophysiology.

2. Materials and methods

2.1. Animals

Six-week-old female C57BL/6 J mice were purchased (CLEA Japan, Inc., Japan). Adolescent female mice were selected because of the high prevalence of AN in females and their greater susceptibility to ABA (Klenotich and Dulawa, 2012). Mice were housed under controlled conditions: inverted 12 h dark-light cycle, dark phase 10:00–22:00 and light phase 22:00–10:00; room temperature (RT): 22 ± 2°C; and relative humidity 50 ± 10 %. Regular food (MF diet; Oriental Yeast Co., Ltd., Japan) was provided. All procedures were conducted in strict accordance with the Policy on the Care and Use of Laboratory Animals, Okayama University. The study protocol was approved by the Animal Care and Use Committee of Okayama University (protocol number: OKU-2024176).

2.2. Generation of ABA mouse model

The protocol for the ABA paradigm was based on instructions by Klenotich and Dulawa (Klenotich and Dulawa, 2012). Mice were randomly assigned to either the ABA or control group. The ABA group mice were individually housed in specialized cages with a running wheel system (Bioseb, France). During the 5-day acclimatization period, the ABA mice had free access to running wheels, food, and water. BW was measured daily at 10:00. At the end of the acclimatization period, we initiated the food restriction (FR) period for the ABA group (FR day 0 [FR0]), in which food was removed from the cage at 12:00 on the same day and stored in separate containers. For the subsequent FR period, ABA mice were provided food for 2 h each day from 10:00–12:00, while maintaining access to running wheels and water. The ABA criterion was defined as BW < 75 % of the baseline (BW measured on FR0). ABA mice meeting these criterion were sacrificed immediately after BW measurement at 10:00. Control mice were kept separately in standard mouse cages, without running wheels, with standard food and water *ad-libitum*; these conditions remained unchanged throughout the experiment. At the conclusion of the experiment (FR7), all remaining ABA mice and control mice were sacrificed. The ABA group mice that did not meet the ABA criteria were excluded. The final analysis included $n = 8$ for the ABA group and $n = 5$ for the control group. Fig. 1 contains summarized animal protocol (Fig. 1**A**) and recorded parameters of the mice (Fig. 1**B-D**), which ABA group showed typical signs of ABA mouse model (Gabloffsky et al., 2022).

2.3. Tissue preparation

The tissue preparation protocol was based on a previous study (Nojima et al., 2021). Mice were anesthetized with isoflurane (262KSQ, Viatris, Japan), followed by blood collection via the abdominal vena cava. Transcardial perfusion was performed with 30 mL of ice-cold phosphate-buffered saline (PBS) followed by 40 mL of 4 % paraformaldehyde (PFA) in PBS for each mouse. Brains were dissected and post-fixed overnight in 4 % PFA in PBS at 4°C, then cryoprotected by incubation in 30 % sucrose in PBS for 48 h at 4°C. The brains were then embedded in optimal cutting temperature compound and frozen. Coronal brain sections (30 μm in thickness) containing mPFC and HPC area were cut using a cryostat (Leica CM1860, Leica Biosystems, Germany), collected in series and preserved at −30°C until immunohistochemistry was performed.

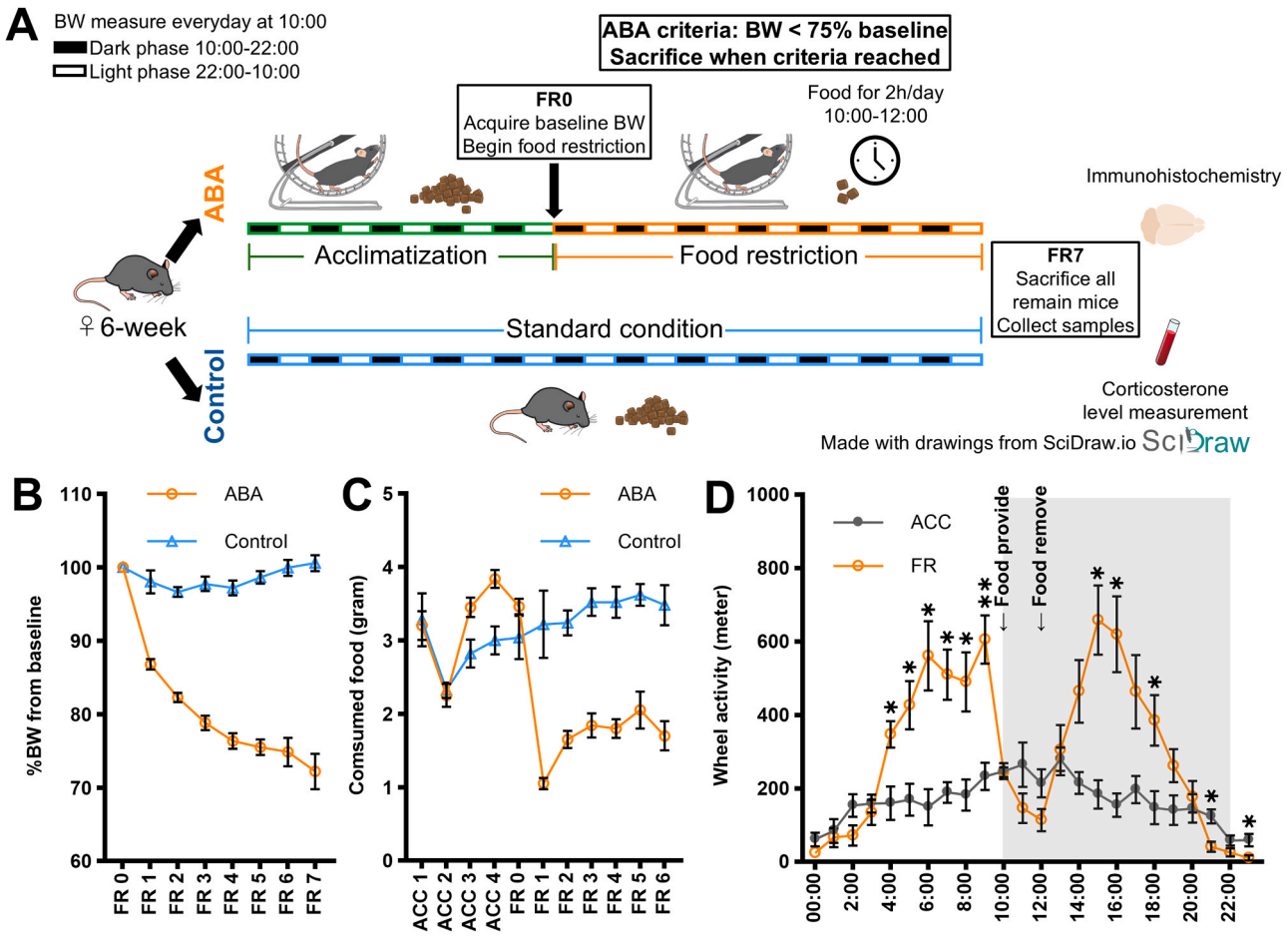

Fig. 1. Generation of ABA mouse model. (A) Schematic for animal experiment. Female mice were divided into ABA and control groups. Mice BW was measured daily at 10:00. ABA mice were provided running wheels, free food and water during acclimatization period, then limited to 2 h of feeding per day (10:00–12:00) from the start of FR period – FR0. ABA group mice reaching ABA criterion (BW < 75 % baseline) were sacrificed after BW measurement. Control group mice were individually housed in standard mouse cages and provided food and water freely throughout the experiment. At FR7, all remaining ABA and control mice were sacrificed. Mice brain and blood samples were collected for analysis. (B) Change of mice BW from baseline and (C) amount of daily consumed food by ABA and control group mice, with ABA mice decreased their BW and food consumption from the start of FR. (D) Diurnal activity transition of ABA group mice during FR, which the mice increased activity level significantly during dark phase (gray background) and light phase (white background) compared to acclimatization period. Each dot represents the mean and error bars represent standard error in each group. Data were analyzed using Mann–Whitney *U* test. Statistical significance is represented by asterisk: * $p < 0.05$, ** $p < 0.01$. BW, bodyweight; ACC, acclimatization; FR, food restriction.

2.4. Corticosterone quantification

Plasma was obtained by centrifugation of whole blood at 845 × g for 15 min at RT, then stored at −80°C. Plasma corticosterone level was measured using a corticosterone enzyme immunoassay kit (cat # ADI-900–097, Enzo Life Sciences, USA). All samples were analyzed in duplicate in a single fluorometry assay using a Multiskan FC microplate photometer (Thermo Fisher, USA), according to the manufacturer's guidelines.

2.5. Immunohistochemistry

For each animal, three brain sections per investigated brain area were randomly selected for staining (mPFC slices: Bregma 1.94–2.1 mm, HPCd slices: Bregma −1.58 to −2.18 mm, HPCv: Bregma −3.28 to −3.40 mm), total number of selected sections for each area: 24 for ABA group, 15 for control group. The sections were washed twice in PBS for 5 min and treated with 0.2 % TritonX-100 in PBS for 10 min at RT. Sections were then washed three times in PBS for 5 min, then incubated with 10 % donkey serum (D9663, Sigma Aldrich, Japan) in PBS for 1 h at RT. After serum solution removal, sections were incubated with rabbit anti-parvalbumin antibody (PV25, Swant, Switzerland, 1:1000) and biotinylated *Wisteria floribunda* agglutinin (WFA) (B-1355, Vector laboratories, USA, 1:100) in PBS overnight at 4°C. After washing in PBS, the sections were incubated with Alexa Fluor 647-conjugated donkey anti-rabbit IgG (ab150075, Abcam, Cambridge, United Kingdom, 1:400) to visualize PV neurons and Alexa Fluor 488-conjugated streptavidin (S11223, Thermo Fisher Scientific, Japan, 1:400) to visualize WFA-stained PNNs [WFA (+) PNNs] in PBS for 2 h at RT. After washing with PBS, the sections were incubated in Neurotrace Nissl 530/615 (N21482, Thermo Fisher Scientific, Japan, 1:200) in 0.03 % TritonX-100 in PBS for 1 h at RT. The sections were then washed in PBS, mounted on glass slides (MAS-01, Matsunami, Japan), dehydrated, cleaned with clean water, and coverslipped using Dako fluorescent mounting medium (S3023, Agilent Technologies, USA).

2.6. Image analysis of PV neurons and WFA (+) PNNs

A confocal microscope (Olympus FV3000, objective lens: 10 ×, numerical aperture 0.4, airy disk × 3) was used to acquire images containing the entire desired analysis area, and the image capture conditions were adjusted to avoid signal saturation and kept constant across images in the same brain area. PolygonAI software (formerly PIPSQUEAK) was used for image analysis, which employs an AI-based

engine allowing automated region of interest (ROI) detection using a preloaded detection model (Slaker et al., 2016). PV neuron and WFA (+) PNN ROIs were marked using PolygonAI in semi-automated mode. Background subtraction was performed across images in the same setting, followed by detection of ROIs using a software preloaded "Parvalbumin" and "WFA" detection model. After automated detection, the ROIs were manually reviewed and corrected. The numbers of annotated PV neuron and WFA (+) PNN ROIs in each group are listed in Supplemental Table. 1. Colocalization between PV neurons and WFA (+) PNNs was detected using the "Colocalize" function in PolygonAI (determined as > 80 % ROI overlap), which was used to classified ROIs into different populations: PV-stained neurons with WFA (+) PNNs enwrapping [PNN (+) PV neurons], PV-stained neurons without WFA (+) PNNs enwrapping [PNN (-) PV neurons], WFA (+) PNNs that enwrap PV neurons [PV (+) PNNs], WFA (+) PNNs that enwrap non-PV stained neurons [PV (-) PNNs]. The exported data from the PolygonAI results files were combined using a custom macro script in FIJI (Schindelin et al., 2012). Regional and layer borders were determined from the Nissl channel using the Van De Werd criteria (Van De Werd et al., 2010) for the mPFC (Fig. 2**A**), and the Reference Mouse Brain Atlas of Allen Brain Atlas (https://atlas.brain-map.org/ n.d.) and Thompson et al. and Dong et al. criteria (Thompson et al., 2008; Dong et al., 2009) for the HPCd and HPCv (Fig. 2**B**, **C**). Table 1 listed the abbreviations of

Table 1
Abbreviations used in figures legends.

Area	Region		Layer	
Medial prefrontal cortex	ILI	Infralimbic	L1	Layer 1
	PLI	Prelimbic	L2/3	Layer 2/3
	dAC	Dorsal anterior cingulate	L5/6	Layer 5/6
	MOs	Secondary motor cortex		
Hippocampus	CA1d	CA1 dorsal	SO	Stratum oriens
	CA3d	CA3 dorsal	SP	Stratum pyramidale
	DeGd	Dentate gyrus dorsal	SR	Stratum radiatum
	CA1v	CA1 ventral	SM	Stratum lacunosum-moleculare
	CA3v	CA3 ventral	MO	Molecular layer
	Subv	Subiculum ventral	SG	Granular layer
			PO	Polymorph layer

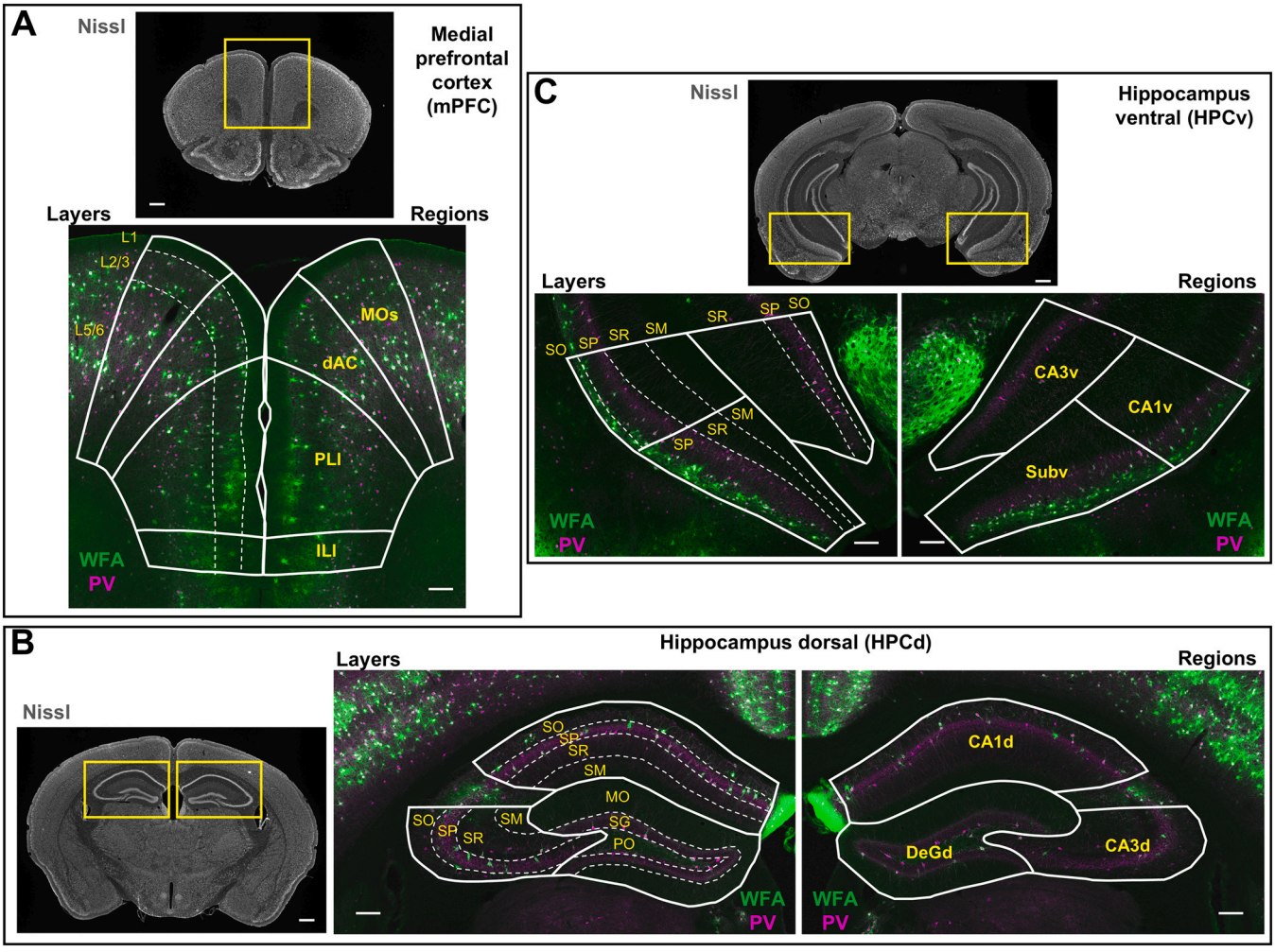

Fig. 2. Representative images of analyzed mouse brain areas and expression of PV and WFA in the brain areas. Representative images of the mPFC (A), HPCd (B), and HPCv (C). Lower magnification images (A and C, top panel; B, left panel) show Nissl-stained image of each brain area. The yellow box indicates the approximate area of the higher magnification images (A and C, bottom panel; B, right panel). Higher magnification images display mouse brain regions and layers. Double staining using PV (magenta) and WFA (green) shows the distribution of PV neurons and WFA (+) PNNs. Scale bar: 500 μm (A and C, top panel; B, left panel) and 200 μm (A and C, bottom panel; B, right panel). See Table 1 for abbreviations.

areas and layers used in figures.

2.7. Data analysis

Data were extracted and calculated from the PolygonAI result files. For expression analysis, the fluorescence intensity of each PV neuron and WFA (+) PNN ROI was calculated as the ROI mean gray value × area; WFA background intensity was subtracted from the fluorescence intensity of each PNN, while no background subtraction was performed for PV neurons because non-specific staining was negligible (Yamada and Jinno, 2013). For density analysis, the density of PV neurons and WFA (+) PNNs in each layer of each region was calculated by dividing the number of detected ROIs by the layer area. The enwrapping status of PV neurons and WFA (+) PNNs was determined from the ROI colocalization results. The average value per mouse was used for group comparisons. Statistical significance between the ABA and control groups was determined using the Mann–Whitney *U* test. Correlations with blood corticosterone level were calculated using Spearman's rank correlation test. Statistical tests were performed using GraphPad Prism 10. *, $p < 0.05$; **, $p < 0.01$; and ***, $p < 0.001$. The statistical threshold was set at $p < 0.05$.

3. Results

3.1. ABA paradigm caused regional PNNs enhancement, while PV neurons were not affected in the mPFC area

We first analyzed PV neurons and WFA (+) PNNs in the mPFC of ABA mice, which was impaired in AN patients. We analyzed layer 2/3 (L2/3) and L5/6 of the mPFC, while L1 was excluded because of the lack of detectable WFA and PV signals (Fig. 3**A**). The ABA mice showed a significant increase in WFA intensity in L2/3 of the prelimbic (PLI), L2/3 of the dorsal anterior cingulate (dAC), and L2/3 and L5/6 of the secondary motor cortex (MOs) compared with control mice (Fig. 3**B**). PNNs density also significantly increased in L2/3 of the PLI and dAC in ABA mice (Fig. 3**C**). However, no significant difference was found in PV intensity (Fig. 3**D**) or PV neuron density (Fig. 3**E**) across all analyzed regions and layers of the mPFC area. These results suggest that the ABA paradigm causes regional PNN enhancement in the mPFC, whereas the PV neurons are generally unaffected.

The ratio of PNNs formed around the PV neurons is another indication of plasticity (Hensch, 2005). The function of PV neurons can change depending on whether they are enwrapped by PNNs, as previously reported for PV neurons in the cortex (Carulli et al., 2010; Hou et al., 2017), and PV neurons lacking PNNs may be more vulnerable (Morishita et al., 2015). Therefore, we separated PV neurons and PNNs based on enwrapping status and investigated whether the ABA paradigm could shift the ratio of PNNs enwrapping PV neurons and its potential effect on each population. We found a minor alteration in the PNN (+) PV neuron ratio over PV neurons and PNNs in ABA mice (Supplementary Fig. 1), suggesting that the distribution of PNN-enwrapped PV neurons was almost unaffected by the ABA paradigm. In the PV (+) PNNs group of ABA mice, there was an increase in WFA intensity in L2/3 of the PLI and L5/6 of the MOs (Fig. 3**F**) but no change in PNN density (Fig. 3**G**). In contrast, in the PV (-) PNNs group, WFA intensity increased in L2/3 of the PLI and dAC (Fig. 3**H**), and a higher PNNs density was observed in L5/6 of the infralimbic (ILI), L2/3 of the PLI, and L2/3 of the dAC in ABA mice (Fig. 3**I**). We found no changes in PV intensity or PV neuron density between ABA and control mice in the PNN (+) and PNN (-) PV neuron groups in individual layers, except for L5/6 of the PLI (Supplementary Fig. 2). Taken together, these results suggest that the ABA paradigm enhances the PNN in PV-negative neurons in the mPFC area, although it does not affect PV neurons whether with or without PNN enwrapping.

3.2. ABA paradigm caused regional PV neurons reduction with PNN alteration in HPCd area

The HPC is another potentially key brain area of ABA pathology, which showed area-specific and differential longitudinal changes in AN patients (Bahnsen et al., 2024); therefore, we next examined the expression and density of PV and WFA in the dorsal part of the HPC in ABA mice. We analyzed each layer of the CA1 dorsal (CA1d), CA3 dorsal (CA3d), and dentate gyrus dorsal (DeGd) regions of the HPCd area, except for the stratum lacunosum-moleculare (SM) layer in the CA1d and CA3d regions because of weak fluorescent signals in both ABA and control mice (Fig. 4**A**). Quantitative analysis showed a significant increase in WFA intensity in the stratum radiatum (SR) layer of CA1, with no significant change in the other layers in ABA mice (Fig. 4**B**). PNN density was higher in the SR but lower in the stratum pyramidale (SP) of CA1d in ABA mice (Fig. 4**C**). The PV intensity was similar between ABA and control mice (Fig. 4**D**), and PV neuron density was reduced in the SP of the CA3d, granular layer (SG), and polymorph layer (PO) of the DeGd in ABA mice (Fig. 4**E**). These findings suggest a layer-dependent PNN alteration and a reduction in the number of regional PV neurons in the HPCd of ABA mice.

Next, we analyzed whether the populations of PNNs and PV neurons were specifically altered in ABA mice. We compared the ratio of PNN (+) PV neurons to the numbers of PV neurons and PNNs between ABA and control mice, which showed no significant change (Supplementary Fig. 3), suggesting that the ABA paradigm did not alter the formation of PNNs enwrapping PV neurons in the HPCd. Analysis of different populations of PNNs showed higher WFA intensity and lower PNN density of PV (+) PNNs in ABA mice than in control mice in the same layers (SP of CA3d and SG of DeGd) (Fig. 4**F**, **G**). We found alterations in WFA intensity in limited layers (SP of CA1d and SG of DeGd) and a higher density of PNN in one layer (SR of CA1d) of PV (-) PNNs (Fig. 4**H**, **I**). These changes in PNNs were not detected in these HPCd regions when the overall PNNs population was analyzed (Fig. 4**B**, **C**). Lower PV neuron density was observed in some layers of both PNN (+) PV neurons (SP of CA3d and SG of DeGd) and PNN (-) PV neurons (SP of CA3d and PO of DeGd) in ABA mice without PV intensity alteration (Supplementary Fig. 4). This result was consistent with the decrease in the total PV neuron density in the same layers (Fig. 4**E**). Together, these results suggest that the ABA paradigm causes a subtle alteration in both PNNs enwrapping PV-positive and PV-negative neurons, and that regional PV neuron reduction is independent of the PNN enwrapping status in the HPCd.

3.3. ABA paradigm caused regional increase in PNN distribution and expression, but not PV neurons in HPCv

Following the analysis of the HPCd, we analyzed the HPCv area to investigate the potential changes in PNNs and PV neurons along the HPC longitudinal axis in ABA mice. We analyzed the CA1 ventral (CA1v), CA3 ventral (CA3v), and subiculum ventral (Subv) regions of the HPCv, excluding the SM layer, since the fluorescent signals of PV and WFA were relatively weak (Fig. 5**A**). PNN changes in the ABA group mice were found in the Subv region: a significant increase in WFA intensity in the SP and SR layers of the Subv (Fig. 5**B**) and a significant increase in PNN density in the SP layer of the Subv (Fig. 5**C**). No significant changes in PNNs were observed for CA1v or CA3v. The PV fluorescence intensity or neuron density remained unchanged throughout the analyzed regions of the HPCv (Fig. 5**D**, **E**). These findings suggest that in the ABA paradigm, PNNs are specifically enhanced in the Subv region, whereas PV neurons are not affected in the HPCv.

Similar to the HPCd, there was no significant difference in the percentage of PNN (+) PV neurons over total PV neuron or total PNN number between ABA and control mice in the HPCd (Supplementary Fig. 5). We analyzed different populations of PNNs, excluding the SR layer in CA1v, stratum oriens layer in CA3v, and SR layer in the Subv

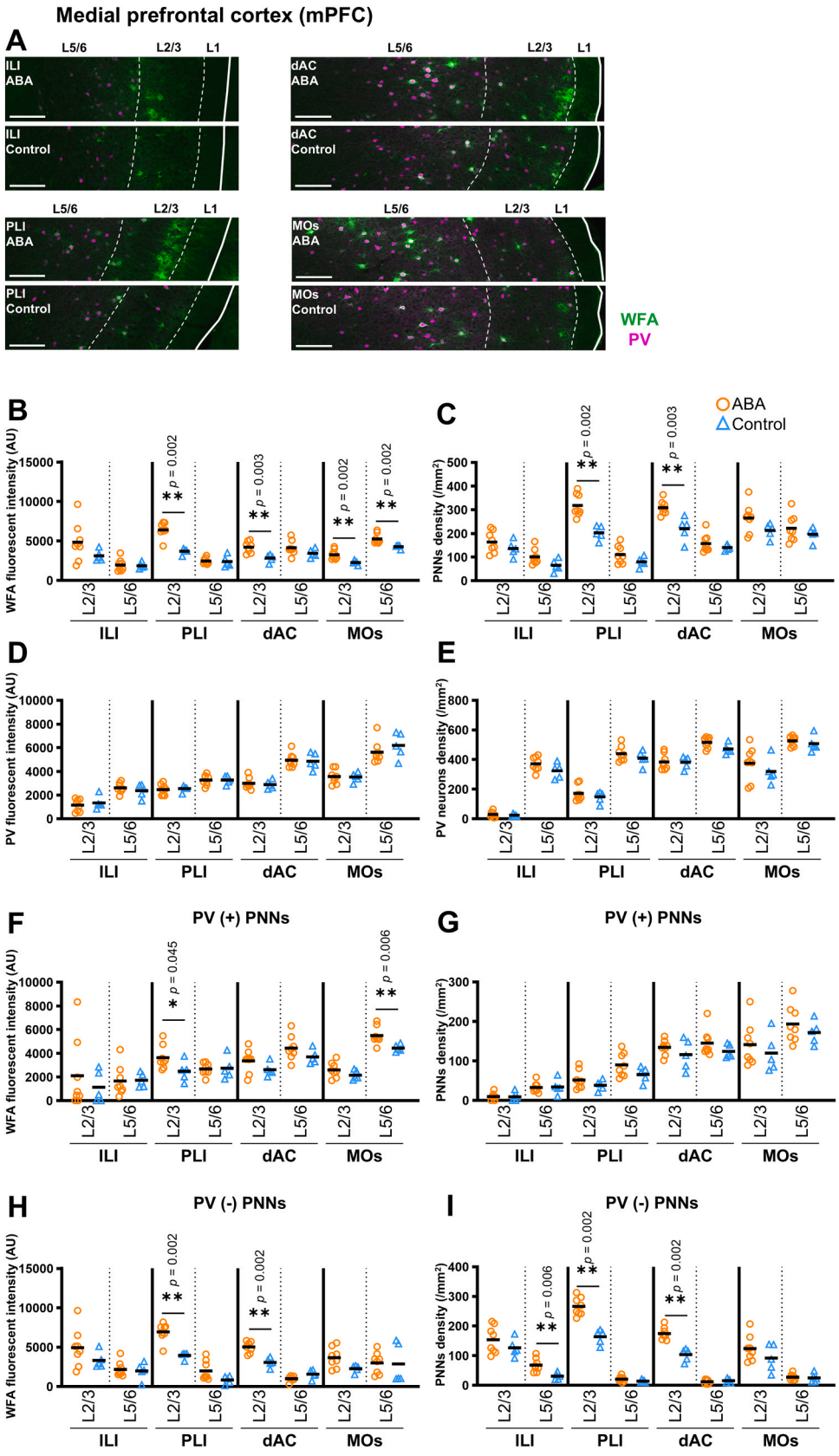

(caption on next page)

Fig. 3. Region-specific analysis of WFA (+) PNN and PV neuron expression and density in mPFC area of ABA mice. (A) Representative images of mPFC regions stained with anti-PV (magenta) and WFA (green) in ABA and control groups. (B-E) The fluorescence intensity of WFA (B) and PV (D), and the density of WFA (+) PNNs (C) and PV neurons (E) in individual layers of the mPFC were compared between ABA and control mice. (F-I) The fluorescence intensity of WFA (F, H) and the density of WFA (+) PNNs (G, I) were analyzed in the PNNs enwrapping PV-positive neuron group (F, G) and PNNs enwrapping PV-negative neuron group (H, I). The expression and density values of individual layers were compared between ABA and control mice. The plotted data are expressed as individual data point for each mouse ($n = 8$ for ABA, $n = 5$ for control). The black bars in each plot represent the mean in each mouse group. Data were analyzed using Mann–Whitney *U* test. Statistical significance is represented by asterisk: * $p < 0.05$, ** $p < 0.01$. See Table 1 for abbreviations.

regions because of the very low PNN count in these layers. In the PV (+) PNN group, WFA intensity was increased in the SP of the Subv (Fig. 5**F**) and PNN density was increased in the SP of the CA3v (Fig. 5**G**) in ABA mice. In the PV (-) PNN group, PNN intensity and density were unchanged between ABA and control mice (Fig. 5**H**, **I**). No changes in PV neurons were found, except for an increase in PV intensity in the SP of CA1v in the PNN (+) PV neuron group and the SP of Subv in the PNN (-) PV neuron group (Supplementary Fig. 6). These findings suggest that PV neuron-enwrapping PNNs preferably contribute to the increase in PNNs expression, and that PV neurons are unaffected in the HPCv of ABA mice.

3.4. ABA paradigm caused an increase in blood corticosterone level, which preferably correlated with the alteration of PNNs

Our results showed that ABA mice had significantly higher blood corticosterone levels than control mice (Fig. 6), suggesting that ABA conditions are stressful for adolescent female mice. To determine the relationship between the increase in corticosterone levels and the alteration of PNNs and PV neurons, we performed a correlation analysis between blood corticosterone levels and WFA (+) PNN and PV neuron expression and density, and the results are listed in Table 2. In the mPFC area, our results showed a significant and strong positive correlation between blood corticosterone levels and WFA fluorescence intensity (in L2/3 of PLI, L2/3 of dAC, and L2/3 and L5/6 of MOs) and PNNs density (in L5/6 of ILI, L2/3 of PLI, and L2/3 of dAC). No significant correlation was found between corticosterone levels and PV neuron fluorescence intensity or density throughout the analyzed regions of the mPFC area. In the HPCd and HPCv areas, only a limited number of analyzed layers showed a significant correlation with corticosterone: positive correlation with WFA intensity in the SR of Subv and SP of CA3v and PNNs density in the SR of CA1d, and negative correlation with PV neuron density in the SP of CA3d. These results suggest that the ABA paradigm causes an elevation in blood corticosterone levels, and there was a strong correlation between corticosterone level increase and the upregulation of PNN expression observed in the mPFC area.

4. Discussion

Our results showed that the ABA paradigm caused a regional enhancement of PNNs in the mPFC area. PNNs expression and density were significantly increased in all analyzed regions of the mPFC, except for the ILI region in the ABA group. PNNs are flexible and their structure and components can shift in response to changes in brain activity (Nakamura et al., 2009; Carulli et al., 2010; McRae et al., 2012). Stress generally causes PNN reduction in the mPFC in animal models (Perlman et al., 2021), however this is usually a result of long-term stress (Gildawie et al., 2021; Ueno et al., 2017a). The seemingly unexpected increase in PNN density in our results might be due to the shorter duration of applied stress (maximum of 7 days under the ABA paradigm). In agreement with this hypothesis, PNNs in the PFC were reported to undergo a biphasic change: the PNN number initially increased on day 7 and then decreased after 35 days of social isolation stress in adolescent male rats (de Araújo Costa Folha et al., 2017). Therefore, it is possible that the PNNs of the mPFC were in an increasing phase when we investigated ABA mouse brains. Interestingly, these newly formed PNNs were likely found around neurons that were not stained with the PV antibody. Further studies are required to identify the type of PNN-bearing neurons and their roles in the pathophysiology of ABA.

In the HPC area, our results show that the ABA paradigm has a region- and layer-specific effect on PNNs, as well as dorsoventral difference. Complex changes in PNNs in the HPC have also been reported in review studies on animal stress models (Laham and Gould, 2022; Perlman et al., 2021). There was a tendency for increased intensity and density of PNNs in the HPC of ABA mice, albeit less obvious than in the mPFC area, therefore HPC plasticity is likely reduced under the acute ABA paradigm, which is consistent with previous reports on HPC plasticity using the ABA model (Chowdhury et al., 2014b, 2014a; Mottarlini et al., 2024). The decrease in PNN density observed in the SP layer of the CA1d could be a result of excessive running in ABA mice, as exercise alone can decrease PNNs density in the CA1d (Terstege et al., 2024), and the CA1 area usually shows early PNN reduction in the stress model (Ueno et al., 2017a; Koskinen et al., 2020). Circadian rhythm is another potential factor. Previous reports have provided evidence of altered circadian rhythm in AN patients (Carollo et al., 2023; Herpertz et al., 1998) and ABA mice (Gabloffsky et al., 2022; Salaün et al., 2024). The mPFC and HPC showed a diurnal rhythm of WFA (+) PNNs density (Pantazopoulos et al., 2020). As ABA mice run much more during the light phase (Beeler et al., 2021; Kuriyama et al., 2023), there is a possibility that the PNNs in the brains of ABA mice have an abnormal rhythm, as shown in our results, as we collected and analyzed brain samples from both ABA and control mice during the same time period.

As for PV neurons, our results showed that PV neurons in the mPFC and HPC areas of the ABA mouse brain were generally not affected. PV interneurons are highly vulnerable to stressors because of their substantial energy requirements, strong excitatory drive, and unique developmental trajectory (Rymar and Sadikot, 2007; Kann et al., 2011; Whittaker et al., 2011; Lu et al., 2014). Generally, stress is one of the main causes of PV neuron vulnerability, as reported from an extensive number of studies: a decrease in PV protein expression in the adolescent mPFC, with little evidence of changes in the HPC, and mixed results in PV neuron density (reviewed by Perlman et al., 2021). The modest reduction in PV neurons in our study can again be related to the duration of the ABA paradigm. PV neuron loss usually occurs after continuous chronic stress (Ueno et al., 2018), or as a sequence of stresses during the early age stage (Cabungcal et al., 2013; Gildawie et al., 2021). In fact, the effect of stress during adolescence on PV interneurons in the mPFC and HPC can be extremely variable, depending on the type of stressor, age at which the animals are exposed, and sex (Perez-Rando et al., 2022). Although not using adolescent age model, the number of PV neurons in the HPC area was reported to decrease after chronic stress, not acute stress in the male rat (Filipović et al., 2013). Therefore, the duration of the ABA paradigm in our study may not have been long enough to manifest a more substantial reduction in PV neurons. Furthermore, there is evidence that chronic stress has a greater impact on PV neurons in the HPCd than in the HPCv (Czéh et al., 2015; Rossetti et al., 2018), which could explain why a reduction in PV neuron number was found in the HPCd but not in the HPCv in our results. Another possibility is that diminishing PV neurons are due to the downregulation of protein markers, which causes them to be undetected by immunohistochemistry rather than neuronal death, and is a region-specific adaptive response against stress (Csabai et al., 2016; Czéh et al., 2018). The alteration of PV neurons observed in our study could be a sign of such a response when the mice were exposed to ABA stress.

We showed that the acute ABA paradigm in adolescent female mice caused a significant increase in blood corticosterone levels, which has

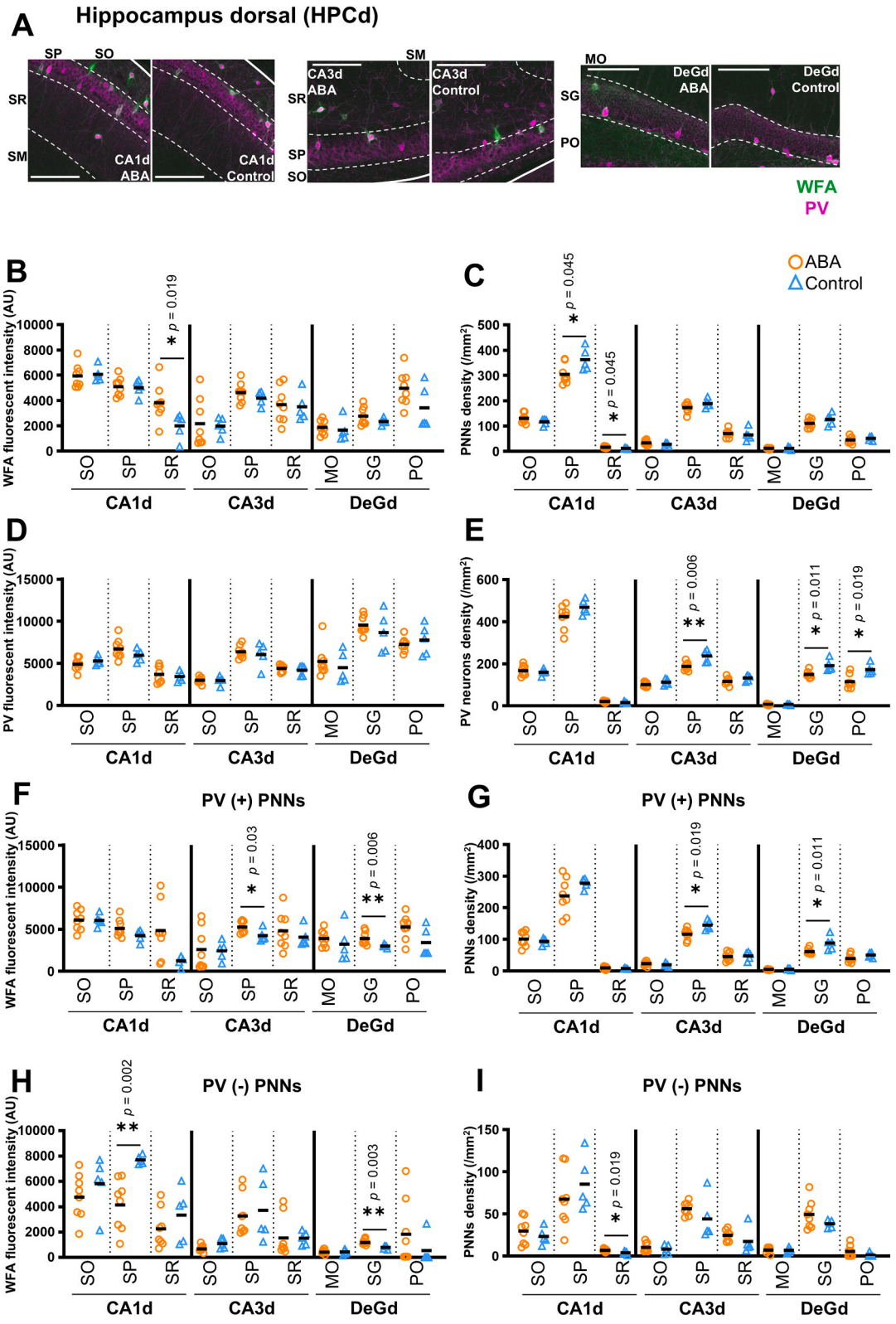

Fig. 4. Region-specific analysis of WFA (+) PNN and PV neuron expression and density in HPCd area of ABA mice. (A) Representative images of HPCd regions stained with anti-PV (Magenta) and WFA (green) in ABA and control groups. (B-E) The fluorescence intensity of WFA (B) and PV (D), and the density of WFA (+) PNNs (C) and PV neurons (E) in individual layers of the HPCd were compared between ABA and control mice. (F-I) The fluorescence intensity of WFA (F, H) and the density of WFA (+) PNNs (G, I) were analyzed in the PNNs enwrapping PV-positive neuron group (F, G) and PNNs enwrapping PV-negative neurons group (H, I). The expression and density values of individual layers were compared between ABA and control mice. The plotted data are expressed as individual data point for each mouse ($n = 8$ for ABA, $n = 5$ for control). The black bars in each plot represent the mean in each mouse group. Data were analyzed using Mann–Whitney U test. Statistical significance is represented by asterisk: * $p < 0.05$, ** $p < 0.01$. See Table 1 for abbreviations.

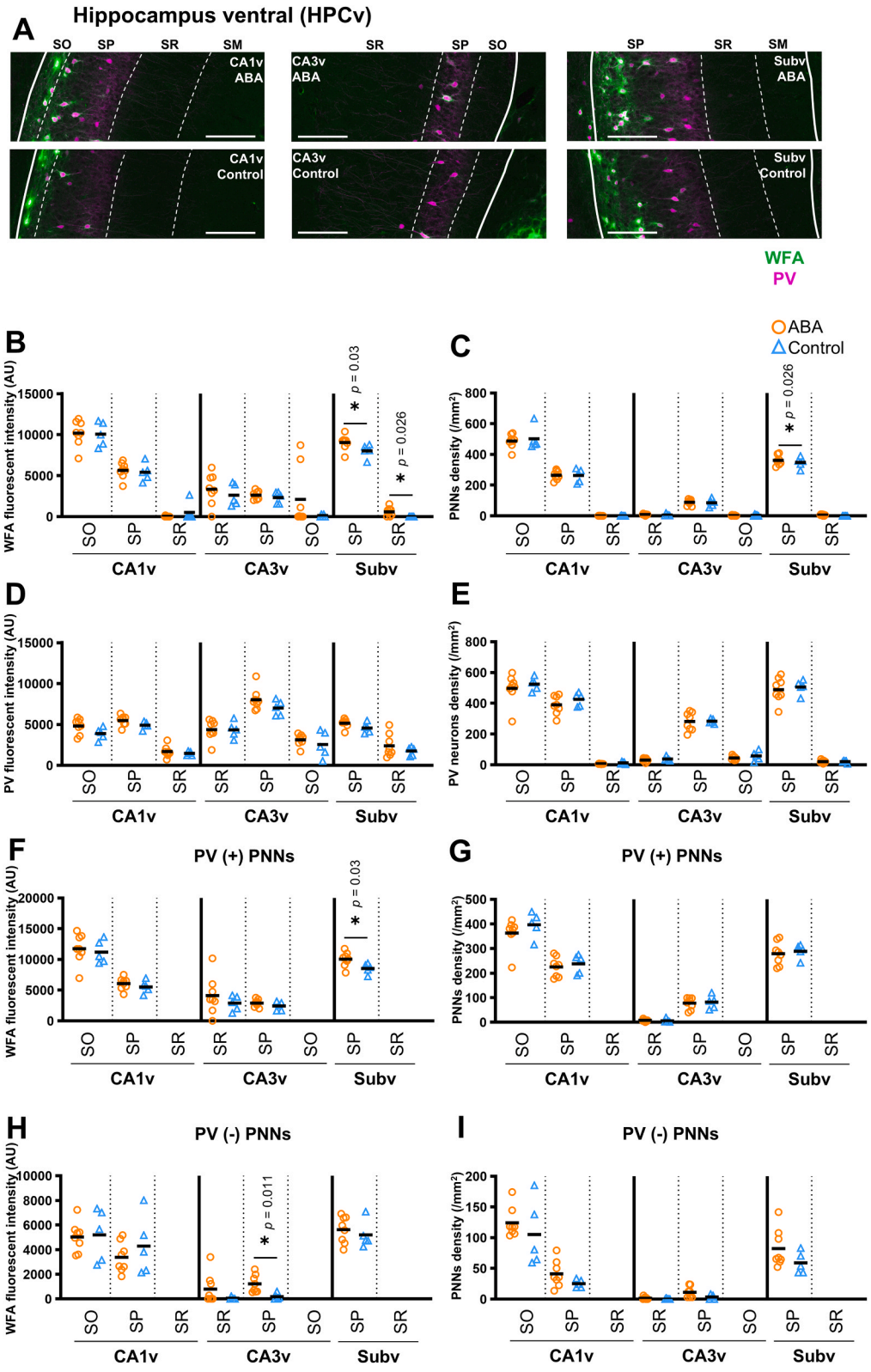

Fig. 5. Region-specific analysis of WFA (+) PNN and PV neuron expression and density in HPCv area of ABA mice. (A) Representative images of HPCv regions stained with anti-PV (magenta) and WFA (green) in ABA and control groups. (B-E) The fluorescence intensity of WFA (B) and PV (D), and density of WFA (+) PNNs (C) and PV neurons (E) in individual layers of the HPCv were compared between ABA and control mice. (F-I) The fluorescence intensity of WFA (F, H) and the density of WFA (+) PNNs (G, I) were analyzed in the PNNs enwrapping PV-positive neuron group (F, G) and PNNs enwrapping PV-negative neurons group (H, I). The expression and density values of individual layers were compared between ABA and control mice. The plotted data are expressed as individual data point for each mouse ($n = 8$ for ABA, $n = 5$ for control). The black bars in each plot represent the mean in each mouse group. Data were analyzed using Mann–Whitney U test. Statistical significance is represented by asterisk: * $p < 0.05$. See Table 1 for abbreviations.

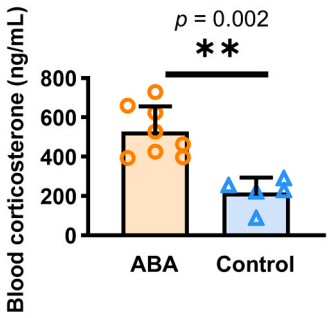

Fig. 6. Blood corticosterone levels in ABA and control mice. Blood corticosterone levels in ABA and control mice were measured and compared. The plotted data are expressed as individual data point for each mouse ($n = 8$ for ABA, $n = 5$ for control). The bar charts in each plot represent the mean, and the error bars represent the standard deviation in each mouse group. Data were analyzed using the Mann–Whitney *U* test. Statistical significance is represented by asterisk: ** $p < 0.01$.

also been reported in previous ABA studies using adolescent animals (Belmonte et al., 2016; Mottarlini et al., 2024). Correlation analysis showed that corticosterone levels were positively correlated with PNN intensity and density in certain PNN populations, focusing on the mPFC. However, no significant correlation was found between corticosterone levels and PV neuron intensity and density in the analyzed areas. These results imply that corticosterone may play a role in regional changes in PNNs and, less likely, PV neurons in the ABA model. Corticoid receptors are abundantly expressed in neurons of the mPFC and HPC (de Kloet et al., 2005; Kraus et al., 2022), both of which show changes in neuronal activity and play a role in regulating glucocorticoid release in response to stress (Mora et al., 2012). PV neuron vulnerability is often accompanied by long-term corticosteroid treatment (Buret and van den Buuse, 2014; Hu et al., 2024); therefore, the shorter duration of increasing corticosterone in the acute ABA paradigm might not cause substantial changes in PV neurons. Acute glucocorticoid treatment may enhance GABAergic transmission in HPC (Hu et al., 2010). It is possible that corticosterone influences PNNs via glial cells, as they can synthesize and break down PNNs components (Crapser et al., 2019; Ribot et al., 2021; Tansley et al., 2022), and there is evidence linking stress and glucocorticoids to glial cell function (Jauregui-Huerta et al., 2010; Tewari et al., 2022). Studies exploring the effect of corticosterone on PNNs in the mPFC and HPC are still lacking; however, corticosterone treatment for 2 weeks resulted in a significant increase in the level of brevican, one of the main PNN components (Favuzzi et al., 2017), and a significant increase in PNN intensity in the HPC (Alaiyed et al., 2020). Further studies are required to uncover the molecular pathway underlying the effect of corticosterone on PV neurons and PNNs.

The main limitation of this study is the lack of characterization and neuronal function analysis, such as neuron subtypes identification, PNN components evaluation, excitatory-inhibitory neurotransmission balance measurement. Therefore, additional investigations such as comprehensive gene expression analysis and evaluation of neural activity are required.

In conclusion, our results demonstrated the effect of the ABA paradigm in adolescent female mice on PNNs, which showed a regional

Table 2
Correlation analysis between blood corticosterone level and the expression and density of WFA (+) PNNs and PV neurons.

mPFC		Correlation with corticosterone level							
		WFA fluorescence intensity		WFA (+) PNN density		PV fluorescence intensity		PV neuron density	
Region	Layer	Spearman r	p	Spearman r	p	Spearman r	p	Spearman r	p
ILI	L2/3	0.451	0.125	0.242	0.426	−0.291	0.334	0.225	0.459
	L5/6	0.099	0.751	0.621*	0.027	0.022	0.949	0.379	0.203
PLI	L2/3	0.769**	0.003	0.852***	0.0004	−0.082	0.793	0.126	0.683
	L5/6	0.341	0.255	0.528	0.067	−0.181	0.554	0.242	0.426
dAC	L2/3	0.753**	0.004	0.775**	0.003	0.368	0.217	0.126	0.683
	L5/6	0.291	0.334	0.181	0.554	0.165	0.591	0.440	0.135
MOs	L2/3	0.830***	0.001	0.539	0.061	0.192	0.529	0.225	0.459
	L5/6	0.659*	0.017	0.242	0.426	−0.055	0.863	0.121	0.696
HPCd		Correlation with corticosterone level							
		WFA fluorescence intensity		WFA (+) PNN density		PV fluorescence intensity		PV neuron density	
Region	Layer	Spearman r	p	Spearman r	p	Spearman r	p	Spearman r	p
CA1d	SO	−0.247	0.415	0.286	0.344	−0.313	0.298	0.137	0.656
	SP	0.033	0.921	−0.550	0.055	0.374	0.210	−0.440	0.135
	SR	0.506	0.081	0.764**	0.003	0.242	0.426	0.555	0.053
CA3d	SO	−0.115	0.710	0.335	0.263	0.258	0.394	−0.110	0.723
	SP	0.176	0.566	−0.368	0.217	0.308	0.306	−0.615*	0.028
	SR	0.077	0.806	0.236	0.437	0.275	0.363	−0.187	0.541
DeGd	MO	−0.038	0.906	−0.225	0.459	0.308	0.306	−0.093	0.765
	SG	0.324	0.280	−0.434	0.141	0.511	0.078	−0.528	0.067
	PO	0.412	0.164	−0.506	0.081	−0.071	0.821	−0.539	0.061
HPCv		Correlation with corticosterone level							
		WFA fluorescence intensity		WFA (+) PNN density		PV fluorescence intensity		PV neuron density	
Region	Layer	Spearman r	p	Spearman r	p	Spearman r	p	Spearman r	p
CA1v	SO	0.027	0.935	0.027	0.935	0.478	0.101	−0.187	0.541
	SP	0.291	0.334	−0.187	0.541	0.390	0.189	−0.467	0.110
	SR	−0.149	0.636	−0.026	0.939	−0.066	0.835	−0.313	0.298
CA3v	SR	0.033	0.921	0.093	0.765	0.165	0.591	−0.220	0.470
	SP	−0.033	0.921	−0.071	0.821	0.566*	0.047	0.005	0.993
	SO	−0.225	0.455	−0.249	0.409	0.286	0.344	−0.324	0.280
Subv	SP	0.517	0.074	−0.033	0.921	0.445	0.130	−0.121	0.696
	SR	0.591*	0.037	0.478	0.102	0.093	0.765	0.093	0.765

Data were analyzed using Spearman's rank correlation test. Statistical significance is represented by asterisk: * $p < 0.05$, ** $p < 0.01$, *** $p < 0.001$. See Table 1 for abbreviations.

increase of PNNs preferably in the mPFC and positively correlated with blood corticosterone level, and PV neurons which were generally unaffected. We hypothesized that these changes represent the adaptive responses of PV neurons and PNNs in the acute phase of stress-driven ABA in mice. Our results provide insights into the roles of PV neurons and PNNs in ABA and AN molecular pathophysiology and their potential as markers for intervention.

Author contributions

H.N. generated the animal model, collected brain samples, performed immunohistochemistry, captured and analyzed images, collected and analyzed data, and wrote the manuscript. H.M. contributed to the analysis method and data validation, and revised the manuscript. H.K. generated the animal model, collected blood samples, and performed corticosterone measurements. Z.W. contributed to the analysis method and revised the manuscript. S.S. provided equipment for the animal experiments and contributed to sample collection. M.T. supervised the project. T.O. supervised the project and revised the manuscript.

CRediT authorship contribution statement

Toshitaka Oohashi: Writing – review & editing, Supervision, Funding acquisition, Conceptualization. **Manabu Takaki:** Supervision. **Shinji Sakamoto:** Resources, Methodology, Conceptualization. **Ziyi Wang:** Writing – review & editing, Methodology. **Hiroki Kawai:** Methodology, Investigation. **Haruko Miyazaki:** Writing – review & editing, Validation, Methodology. **Hoang Duy Nguyen:** Writing – original draft, Methodology, Investigation, Formal analysis.

Declaration of Competing Interest

The authors declare no conflicts of interest.

Acknowledgement

We would like to thank MS. Nanami Wada for assisting with tissue collection, and Prof. Ayano Kawaguchi and Dr. Atsunori Shitamukai for their technical assistance with confocal microscopy. We would like to thank Editage (www.editage.jp) for English language editing. We thank SciDraw.io for providing the illustrations. We are also grateful to the members of the Molecular Biology and Biochemistry Department, Okayama University Graduate School of Medicine, Dentistry, and Pharmaceutical Sciences, Okayama, for their valuable assistance with this paper. This work was funded by the following grants: KAKENHI 23H04235, 24K10733, and 24KK0155 (to T.O.).

Appendix A. Supporting information

Supplementary data associated with this article can be found in the online version at doi:10.1016/j.neures.2025.104922.

References

Ährlund-Richter, S., Xuan, Y., van Lunteren, J.A., Kim, H., Ortiz, C., Pollak Dorocic, I., Meletis, K., Carlén, M., 2019. A whole-brain atlas of monosynaptic input targeting four different cell types in the medial prefrontal cortex of the mouse. Nat. Neurosci. 22, 657–668. https://doi.org/10.1038/s41593-019-0354-y.

Alaiyed, S., McCann, M., Mahajan, G., Rajkowska, G., Stockmeier, C.A., Kellar, K.J., Wu, J.Y., Conant, K., 2020. Venlafaxine Stimulates an MMP-9-Dependent Increase in Excitatory/Inhibitory Balance in a Stress Model of Depression. J. Neurosci. 40, 4418. https://doi.org/10.1523/JNEUROSCI.2387-19.2020.

American Psychiatric Association, 2013. Diagn. Stat. Man. Ment. Disord. 5th ed.).

Bahnsen, K., Wronski, M.-L., Keeler, J.L., King, J.A., Preusker, Q., Kolb, T., Weidner, K., Roessner, V., Bernardoni, F., Ehrlich, S., 2024. Differential longitudinal changes of hippocampal subfields in patients with anorexia nervosa. Psychiatry Clin. Neurosci. 78, 186–196. https://doi.org/10.1111/pcn.13626.

Balmer, T.S., 2016. Perineuronal Nets Enhance the Excitability of Fast-Spiking Neurons. eNeuro 3. https://doi.org/10.1523/ENEURO.0112-16.2016.

Bannerman, D.M., Rawlins, J.N.P., McHugh, S.B., Deacon, R.M.J., Yee, B.K., Bast, T., Zhang, W.-N., Pothuizen, H.H.J., Feldon, J., 2004. Regional dissociations within the hippocampus—memory and anxiety (Anxiety and Neuroticism). Neurosci. Biobehav. Rev. Festschr. Honour Jeffrey Gray 28 (1), 273–283. https://doi.org/10.1016/j.neubiorev.2004.03.004.

Beeler, J.A., Mourra, D., Zanca, R.M., Kalmbach, A., Gellman, C., Klein, B.Y., Ravenelle, R., Serrano, P., Moore, H., Rayport, S., Mingote, S., Burghardt, N.S., 2021. VULNERABLE AND RESILIENT PHENOTYPES IN A MOUSE MODEL OF ANOREXIA NERVOSA. Biol. Psychiatry 90, 829–842. https://doi.org/10.1016/j.biopsych.2020.06.030.

Belmonte, L., Achamrah, N., Nobis, S., Guérin, C., Riou, G., Bôle-Feysot, C., Boyer, O., Richard, V., Rego, J.C.D., Déchelotte, P., Goichon, A., Coëffier, M., 2016. A role for intestinal TLR4-driven inflammatory response during activity-based anorexia. Sci. Rep. 6, 35813. https://doi.org/10.1038/srep35813.

Beurdeley, M., Spatazza, J., Lee, H.H.C., Sugiyama, S., Bernard, C., Nardo, A.A.D., Hensch, T.K., Prochiantz, A., 2012. Otx2 Binding to Perineuronal Nets Persistently Regulates Plasticity in the Mature Visual Cortex. J. Neurosci. 32, 9429–9437. https://doi.org/10.1523/JNEUROSCI.0394-12.2012.

Bittar, T.P., Labonté, B., 2021. Functional Contribution of the Medial Prefrontal Circuitry in Major Depressive Disorder and Stress-Induced Depressive-Like Behaviors. Front. Behav. Neurosci. 15. https://doi.org/10.3389/fnbeh.2021.699592.

Brockmeyer, T., Friederich, H.-C., Schmidt, U., 2018. Advances in the treatment of anorexia nervosa: a review of established and emerging interventions. Psychol. Med. 48, 1228–1256. https://doi.org/10.1017/S0033291717002604.

Buret, L., van den Buuse, M., 2014. Corticosterone treatment during adolescence induces down-regulation of reelin and NMDA receptor subunit GLUN2C expression only in male mice: implications for schizophrenia. Int. J. Neuropsychopharmacol. 17, 1221–1232. https://doi.org/10.1017/S1461145714000121.

Burkert, N.T., Koschutnig, K., Ebner, F., Freidl, W., 2015. Structural hippocampal alterations, perceived stress, and coping deficiencies in patients with anorexia nervosa. Int. J. Eat. Disord. 48, 670–676. https://doi.org/10.1002/eat.22397.

Cabungcal, J.-H., Steullet, P., Morishita, H., Kraftsik, R., Cuenod, M., Hensch, T.K., Do, K. Q., 2013. Perineuronal nets protect fast-spiking interneurons against oxidative stress. Proc. Natl. Acad. Sci. 110, 9130–9135. https://doi.org/10.1073/pnas.1300454110.

Carollo, A., Zhang, P., Yin, P., Jawed, A., Dimitriou, D., Esposito, G., Mangar, S., 2023. Sleep Profiles in Eating Disorders: A Scientometric Study on 50 Years of Clinical Research. Healthcare 11, 2090. https://doi.org/10.3390/healthcare11142090.

Carulli, D., Broersen, R., de Winter, F., Muir, E.M., Mešković, M., de Waal, M., de Vries, S., Boele, H.-J., Canto, C.B., De Zeeuw, C.I., Verhaagen, J., 2020. Cerebellar plasticity and associative memories are controlled by perineuronal nets. Proc. Natl. Acad. Sci. 117, 6855–6865. https://doi.org/10.1073/pnas.1916163117.

Carulli, D., Pizzorusso, T., Kwok, J.C.F., Putignano, E., Poli, A., Forostyak, S., Andrews, M.R., Deepa, S.S., Glant, T.T., Fawcett, J.W., 2010. Animals lacking link protein have attenuated perineuronal nets and persistent plasticity. Brain 133, 2331–2347. https://doi.org/10.1093/brain/awq145.

Champagne, D.L., Bagot, R.C., Hasselt, van, F., Ramakers, Meaney, G., Kloet, M.J., de, E. R., Joëls, M., Krugers, H., 2008. Maternal Care and Hippocampal Plasticity: Evidence for Experience-Dependent Structural Plasticity, Altered Synaptic Functioning, and Differential Responsiveness to Glucocorticoids and Stress. J. Neurosci. 28, 6037–6045. https://doi.org/10.1523/JNEUROSCI.0526-08.2008.

Charrat, J.-P., Massoubre, C., Germain, N., Gay, A., Galusca, B., 2023. Systematic review of prospective studies assessing risk factors to predict anorexia nervosa onset. J. Eat. Disord. 11, 163. https://doi.org/10.1186/s40337-023-00882-0.

Chowdhury, T.G., Barbarich-Marsteller, N.C., Chan, T.E., Aoki, C., 2014a. Activity-based anorexia has differential effects on apical dendritic branching in dorsal and ventral hippocampal CA1. Brain Struct. Funct. 219, 1935. https://doi.org/10.1007/s00429-013-0612-9.

Chowdhury, T.G., Ríos, M.B., Chan, T.E., Cassataro, D.S., Barbarich-Marsteller, N.C., Aoki, C., 2014b. Activity-based anorexia during adolescence disrupts normal development of the CA1 pyramidal cells in the ventral hippocampus of female rats. Hippocampus 24, 1421–1429. https://doi.org/10.1002/hipo.22320.

Crapser, J.D., Ochaba, J., Soni, N., Reidling, J.C., Thompson, L.M., Green, K.N., 2019. Microglial depletion prevents extracellular matrix changes and striatal volume reduction in a model of Huntington's disease. Brain 143, 266. https://doi.org/10.1093/brain/awz363.

Csabai, D., Seress, L., Varga, Z., Ábrahám, H., Miseta, A., Wiborg, O., Czéh, B., 2016. Electron Microscopic Analysis of Hippocampal Axo-Somatic Synapses in a Chronic Stress Model for Depression. Hippocampus 27, 17. https://doi.org/10.1002/hipo.22650.

Czéh, B., Vardya, I., Varga, Z., Febbraro, F., Csabai, D., Martis, L.-S., Højgaard, K., Henningsen, K., Bouzinova, E.V., Miseta, A., Jensen, K., Wiborg, O., 2018. Long-Term Stress Disrupts the Structural and Functional Integrity of GABAergic Neuronal Networks in the Medial Prefrontal Cortex of Rats. Front. Cell. Neurosci. 12, 148. https://doi.org/10.3389/fncel.2018.00148.

Czéh, B., Varga, Z.K.K., Henningsen, K., Kovács, G.L., Miseta, A., Wiborg, O., 2015. Chronic stress reduces the number of GABAergic interneurons in the adult rat hippocampus, dorsal-ventral and region-specific differences. Hippocampus 25, 393–405. https://doi.org/10.1002/hipo.22382.

de Araújo Costa Folha, O.A., Bahia, C.P., de Aguiar, G.P.S., Herculano, A.M., Coelho, N.L. G., de Sousa, M.B.C., Shiramizu, V.K.M., de Menezes Galvão, A.C., de Carvalho, W. A., Pereira, A., 2017. Effect of chronic stress during adolescence in prefrontal cortex structure and function. Behav. Brain Res. 326, 44–51. https://doi.org/10.1016/j.bbr.2017.02.033.

de Kloet, E.R., Joëls, M., Holsboer, F., 2005. Stress and the brain: from adaptation to disease. Nat. Rev. Neurosci. 6, 463–475. https://doi.org/10.1038/nrn1683.
de Vivo, L., Landi, S., Panniello, M., Baroncelli, L., Chierzi, S., Mariotti, L., Spolidoro, M., Pizzorusso, T., Maffei, L., Ratto, G.M., 2013. Extracellular matrix inhibits structural and functional plasticity of dendritic spines in the adult visual cortex. Nat. Commun. 4, 1484. https://doi.org/10.1038/ncomms2491.
Dick, G., Tan, C.L., Alves, J.N., Ehlert, E.M.E., Miller, G.M., Hsieh-Wilson, L.C., Sugahara, K., Oosterhof, A., van Kuppevelt, T.H., Verhaagen, J., Fawcett, J.W., Kwok, J.C.F., 2013. Semaphorin 3A Binds to the Perineuronal Nets via Chondroitin Sulfate Type E Motifs in Rodent Brains. J. Biol. Chem. 288, 27384–27395. https://doi.org/10.1074/jbc.M111.310029.
Dityatev, A., Brückner, G., Dityateva, G., Grosche, J., Kleene, R., Schachner, M., 2007. Activity-dependent formation and functions of chondroitin sulfate-rich extracellular matrix of perineuronal nets. Dev. Neurobiol. 67, 570–588. https://doi.org/10.1002/dneu.20361.
Dong, H.-W., Swanson, L.W., Chen, L., Fanselow, M.S., Toga, A.W., 2009. Genomic–anatomic evidence for distinct functional domains in hippocampal field CA1. Proc. Natl. Acad. Sci. 106, 11794–11799. https://doi.org/10.1073/pnas.0812608106.
Fanselow, M.S., Dong, H.-W., 2010. Are The Dorsal and Ventral Hippocampus functionally distinct structures? Neuron 65, 7. https://doi.org/10.1016/j.neuron.2009.11.031.
Favuzzi, E., Marques-Smith, A., Deogracias, R., Winterflood, C.M., Sánchez-Aguilera, A., Mantoan, L., Maeso, P., Fernandes, C., Ewers, H., Rico, B., 2017. Activity-Dependent Gating of Parvalbumin Interneuron Function by the Perineuronal Net Protein Brevican. Neuron 95, 639–655.e10. https://doi.org/10.1016/j.neuron.2017.06.028.
Fawcett, J.W., Oohashi, T., Pizzorusso, T., 2019. The roles of perineuronal nets and the perinodal extracellular matrix in neuronal function. Nat. Rev. Neurosci. 20, 451–465. https://doi.org/10.1038/s41583-019-0196-3.
Ferguson, B.R., Gao, W.-J., 2018. PV Interneurons: Critical Regulators of E/I Balance for Prefrontal Cortex-Dependent Behavior and Psychiatric Disorders. Front. Neural Circuits 12, 37. https://doi.org/10.3389/fncir.2018.00037.
Filipović, D., Zlatković, J., Gass, P., Inta, D., 2013. The differential effects of acute vs. chronic stress and their combination on hippocampal parvalbumin and inducible heat shock protein 70 expression. Neuroscience 236, 47–54. https://doi.org/10.1016/j.neuroscience.2013.01.033.
Foldi, C.J., 2024. Taking better advantage of the activity-based anorexia model (Special issue: Eating disorders). Trends Mol. Med. 30, 330–338. https://doi.org/10.1016/j.molmed.2023.11.011.
Fuglset, T.S., Landrø, N.I., Reas, D.L., Rø, Ø., 2016. Functional brain alterations in anorexia nervosa: a scoping review. J. Eat. Disord. 4, 32. https://doi.org/10.1186/s40337-016-0118-y.
Gabloffsky, T., Gill, S., Staffeld, A., Salomon, R., Guerra, N.P., Joost, S., Hawlitschka, A., Kipp, M., Frintrop, L., 2022. Food Restriction in Mice Induces Food-Anticipatory Activity and Circadian-Rhythm-Related Activity Changes. Nutrients 14, 5252. https://doi.org/10.3390/nu14245252.
Gildawie, K.R., Ryll, L.M., Hexter, J.C., Peterzell, S., Valentine, A.A., Brenhouse, H.C., 2021. A two-hit adversity model in developing rats reveals sex-specific impacts on prefrontal cortex structure and behavior. Dev. Cogn. Neurosci. 48, 100924. https://doi.org/10.1016/j.dcn.2021.100924.
Gould, E., Tanapat, P., 1999. Stress and hippocampal neurogenesis. Biol. Psychiatry 46, 1472–1479. https://doi.org/10.1016/S0006-3223(99)00247-4.
Happel, M.F.K., Niekisch, H., Castiblanco Rivera, L.L., Ohl, F.W., Deliano, M., Frischknecht, R., 2014. Enhanced cognitive flexibility in reversal learning induced by removal of the extracellular matrix in auditory cortex. Proc. Natl. Acad. Sci. 111, 2800–2805. https://doi.org/10.1073/pnas.1310272111.
Hensch, T.K., 2005. Critical period plasticity in local cortical circuits. Nat. Rev. Neurosci. 6, 877–888. https://doi.org/10.1038/nrn1787.
Herpertz, S., Wagner, R., Albers, N., Blum, W.F., Pelz, B., Langkafel, M., Köpp, W., Henning, A., Oberste-Berghaus, C., Mann, K., Senf, W., Hebebrand, J., 1998. Circadian Plasma Leptin Levels in Patients with Anorexia nervosa: Relation to Insulin and Cortisol. Horm. Res. 50, 197–204. https://doi.org/10.1159/000023274.
Hou, X., Yoshioka, N., Tsukano, H., Sakai, A., Miyata, S., Watanabe, Y., Yanagawa, Y., Sakimura, K., Takeuchi, K., Kitagawa, H., Hensch, T.K., Shibuki, K., Igarashi, M., Sugiyama, S., 2017. Chondroitin Sulfate Is Required for Onset and Offset of Critical Period Plasticity in Visual Cortex. Sci. Rep. 7, 12646. https://doi.org/10.1038/s41598-017-04007-x.
https://atlas.brain-map.org/ [WWW Document], n.d.. Allen Ref. Atlas – Mouse Brain Brain Atlas Available Atlasbrain-Maporg. URL https://atlas.brain-map.org/.
Hu, H., Gan, J., Jonas, P., 2014. Fast-spiking, parvalbumin+ GABAergic interneurons: From cellular design to microcircuit function. Science 345, 1255263. https://doi.org/10.1126/science.1255263.
Hu, L., Qiu, M.-J., Fan, W.-J., Wang, W.-E., Liu, S.-H., Liu, X.-Q., Liu, S.-W., Shen, Z.-J., Zheng, Y.-F., Liu, G.-C., Jia, Z.-Y., Wang, X.-Q., Fang, N., 2024. Characterization of GABAergic marker expression in prefrontal cortex in dexamethasone induced depression/anxiety model. Front. Endocrinol. 15, 1433026. https://doi.org/10.3389/fendo.2024.1433026.
Hu, W., Zhang, M., Czéh, B., Flügge, G., Zhang, W., 2010. Stress Impairs GABAergic Network Function in the Hippocampus by Activating Nongenomic Glucocorticoid Receptors and Affecting the Integrity of the Parvalbumin-Expressing Neuronal Network. Neuropsychopharmacology 35, 1693–1707. https://doi.org/10.1038/npp.2010.31.
Jauregui-Huerta, F., Ruvalcaba-Delgadillo, Y., Gonzalez-Perez, O., Gonzalez-Castaneda, R., Garcia-Estrada, J., Luquin, S., 2010. Responses of Glial Cells to Stress and Glucocorticoids. Curr. Immunol. Rev. Discontin. 6, 195–204. https://doi.org/10.2174/157339510791823790.
Kann, O., Huchzermeyer, C., Kovács, R., Wirtz, S., Schuelke, M., 2011. Gamma oscillations in the hippocampus require high complex I gene expression and strong functional performance of mitochondria. Brain 134, 345–358. https://doi.org/10.1093/brain/awq333.
Keeler, J., Patsalos, O., Thuret, S., Ehrlich, S., Tchanturia, K., Himmerich, H., Treasure, J., 2020. Hippocampal volume, function, and related molecular activity in anorexia nervosa: A scoping review. Expert Rev. Clin. Pharm. 13, 1367–1387. https://doi.org/10.1080/17512433.2020.1850256.
Khalsa, S.S., Portnoff, L.C., McCurdy-McKinnon, D., Feusner, J.D., 2017. What happens after treatment? A systematic review of relapse, remission, and recovery in anorexia nervosa. J. Eat. Disord. 5, 20. https://doi.org/10.1186/s40337-017-0145-3.
Klenotich, S.J., Dulawa, S.C., 2012. The Activity-Based Anorexia Mouse Model. In: Kobeissy, F.H. (Ed.), Psychiatric Disorders: Methods and Protocols, Methods in Molecular Biology. Humana Press, Totowa, NJ, pp. 377–393. https://doi.org/10.1007/978-1-61779-458-2_25.
Koskinen, M.-K., van Mourik, Y., Smit, A.B., Riga, D., Spijker, S., 2020. From stress to depression: development of extracellular matrix-dependent cognitive impairment following social stress. Sci. Rep. 10, 17308. https://doi.org/10.1038/s41598-020-73173-2.
Kraus, K.L., Chordia, A.P., Drake, A.W., Herman, J.P., Danzer, S.C., 2022. Hippocampal interneurons are direct targets for circulating glucocorticoids. J. Comp. Neurol. 530, 2100–2112. https://doi.org/10.1002/cne.25322.
Kuriyama, T., Murata, Y., Ohtani, R., Yahara, R., Nakashima, S., Mori, M., Ohe, K., Mine, K., Enjoji, M., 2023. Modified activity-based anorexia paradigm dampens chronic food restriction-induced hyperadiponectinemia in adolescent female mice. PLOS ONE 18, e0289020. https://doi.org/10.1371/journal.pone.0289020.
Laham, B.J., Gould, E., 2022. How Stress Influences the Dynamic Plasticity of the Brain's Extracellular Matrix. Front. Cell. Neurosci. 15, 814287. https://doi.org/10.3389/fncel.2021.814287.
Lamanna, J., Isotti, F., Ferro, M., Racchetti, G., Anchora, L., Rucco, D., Malgaroli, A., 2021. Facilitation of dopamine-dependent long-term potentiation in the medial prefrontal cortex of male rats follows the behavioral effects of stress. J. Neurosci. Res. 99, 662–678. https://doi.org/10.1002/jnr.24732.
Lawson, E.A., Donoho, D., Miller, K.K., Misra, M., Meenaghan, E., Lydecker, J., Wexler, T., Herzog, D.B., Klibanski, A., 2009. Hypercortisolemia Is Associated with Severity of Bone Loss and Depression in Hypothalamic Amenorrhea and Anorexia Nervosa. J. Clin. Endocrinol. Metab. 94, 4710. https://doi.org/10.1210/jc.2009-1046.
Le Merre, P., Ährlund-Richter, S., Carlén, M., 2021. The mouse prefrontal cortex: Unity in diversity. Neuron 109, 1925–1944. https://doi.org/10.1016/j.neuron.2021.03.035.
Lu, J., Tucciarone, J., Lin, Y., Huang, Z.J., 2014. Input-specific maturation of synaptic dynamics of parvalbumin interneurons in primary visual cortex. Proc. Natl. Acad. Sci. 111, 16895–16900. https://doi.org/10.1073/pnas.1400694111.
Lupori, L., Totaro, V., Cornuti, S., Ciampi, L., Carrara, F., Grilli, E., Viglione, A., Tozzi, F., Putignano, E., Mazziotti, R., Amato, G., Gennaro, C., Tognini, P., Pizzorusso, T., 2023. A Compr. Atlas Perineuronal Net. Distrib. Coloca. Parvalbumin Adult Mouse Brain. https://doi.org/10.1101/2023.01.24.525313.
Luz Neto, L.M., da, Vasconcelos, F.M.N., de, Silva, J.E., da, Pinto, T.C.C., Sougey, É.B., Ximenes, R.C.C., 2019. Differences in cortisol concentrations in adolescents with eating disorders: a systematic review. J. Pediatr. (Rio J.) 95, 18–26. https://doi.org/10.1016/j.jped.2018.02.007.
Maroun, M., Richter-Levin, G., 2003. Exposure to Acute Stress Blocks the Induction of Long-Term Potentiation of the Amygdala–Prefrontal Cortex Pathway In Vivo. J. Neurosci. 23, 4406. https://doi.org/10.1523/JNEUROSCI.23-11-04406.2003.
McRae, P.A., Baranov, E., Rogers, S.L., Porter, B.E., 2012. Persistent decrease in multiple components of the perineuronal net following status epilepticus. Eur. J. Neurosci. 36, 3471. https://doi.org/10.1111/j.1460-9568.2012.08268.x.
Melissa, R., Lama, M., Laurence, K., Sylvie, B., Jeanne, D., Odile, V., Nathalie, G., 2020. Physical Activity in Eating Disorders: A Systematic Review. Nutrients 12, 183. https://doi.org/10.3390/nu12010183.
Misra, M., Miller, K.K., Almazan, C., Ramaswamy, K., Lapcharoensap, W., Worley, M., Neubauer, G., Herzog, D.B., Klibanski, A., 2004. Alterations in Cortisol Secretory Dynamics in Adolescent Girls with Anorexia Nervosa and Effects on Bone Metabolism. J. Clin. Endocrinol. Metab. 89, 4972–4980. https://doi.org/10.1210/jc.2004-0723.
Misra, M., Prabhakaran, R., Miller, K.K., Tsai, P., Lin, A., Lee, N., Herzog, D.B., Klibanski, A., 2006. Role of Cortisol in Menstrual Recovery in Adolescent Girls with Anorexia Nervosa. Pediatr. Res. 59, 598–603. https://doi.org/10.1203/01.pdr.0000203097.64918.63.
Miyata, S., Kitagawa, H., 2015. Mechanisms for modulation of neural plasticity and axon regeneration by chondroitin sulphate. J. Biochem. (Tokyo) 157, 13–22. https://doi.org/10.1093/jb/mvu067.
Mora, F., Segovia, G., del Arco, A., de Blas, M., Garrido, P., 2012. Stress, neurotransmitters, corticosterone and body–brain integration (Brain Integration - from Molecular to Network Level). Brain Res 1476, 71–85. https://doi.org/10.1016/j.brainres.2011.12.049.
Morawski, M., Reinert, T., Meyer-Klaucke, W., Wagner, F.E., Tröger, W., Reinert, A., Jäger, C., Brückner, G., Arendt, T., 2015. Ion exchanger in the brain: Quantitative analysis of perineuronally fixed anionic binding sites suggests diffusion barriers with ion sorting properties. Sci. Rep. 5, 16471. https://doi.org/10.1038/srep16471.
Morishita, H., Cabungcal, J.-H., Chen, Y., Do, K.Q., Hensch, T.K., 2015. Prolonged Period of Cortical Plasticity upon Redox Dysregulation in Fast-Spiking Interneurons. Biol. Psychiatry Mol. Mech. Synaptic Deficits Schizophr. 78, 396–402. https://doi.org/10.1016/j.biopsych.2014.12.026.
Mottarlini, F., Targa, G., Rizzi, B., Fumagalli, F., Caffino, L., 2024. Developmental activity-based anorexia alters hippocampal non-genomic stress response and induces

structural instability and spatial memory impairment in female rats. Prog. Neuropsychopharmacol. Biol. Psychiatry 134, 111065. https://doi.org/10.1016/j.pnpbp.2024.111065.
Nakamura, M., Nakano, K., Morita, S., Nakashima, T., Oohira, A., Miyata, S., 2009. Expression of chondroitin sulfate proteoglycans in barrel field of mouse and rat somatosensory cortex. Brain Res 1252, 117–129. https://doi.org/10.1016/j.brainres.2008.11.022.
Nojima, K., Miyazaki, H., Hori, T., Vargova, L., Oohashi, T., 2021. Assessment of Possible Contributions of Hyaluronan and Proteoglycan Binding Link Protein 4 to Differential Perineuronal Net Formation at the Calyx of Held. Front. Cell Dev. Biol. 9, 730550. https://doi.org/10.3389/fcell.2021.730550.
Oohashi, T., Edamatsu, M., Bekku, Y., Carulli, D., 2015. The hyaluronan and proteoglycan link proteins: Organizers of the brain extracellular matrix and key molecules for neuronal function and plasticity. Exp. Neurol. 274, 134–144. https://doi.org/10.1016/j.expneurol.2015.09.010.
Packer, A.M., Yuste, R., 2011. Dense, Unspecific Connectivity of Neocortical Parvalbumin-Positive Interneurons: A Canonical Microcircuit for Inhibition? J. Neurosci. 31, 13260. https://doi.org/10.1523/JNEUROSCI.3131-11.2011.
Pantazopoulos, H., Berretta, S., 2016. In Sickness and in Health: Perineuronal Nets and Synaptic Plasticity in Psychiatric Disorders. Neural Plast. 2016, 9847696. https://doi.org/10.1155/2016/9847696.
Pantazopoulos, H., Gisabella, B., Rexrode, L., Benefield, D., Yildiz, E., Seltzer, P., Valeri, J., Chelini, G., Reich, A., Ardelt, M., Berretta, S., 2020. Circadian Rhythms of Perineuronal Net Composition. eNeuro 7. https://doi.org/10.1523/ENEURO.0034-19.2020.
Perez-Rando, M., Carceller, H., Castillo-Gomez, E., Bueno-Fernandez, C., García-Mompó, C., Gilabert-Juan, J., Guirado, R., Pesarico, A.P., Nacher, J., 2022. Impact of stress on inhibitory neuronal circuits, our tribute to Bruce McEwen. Neurobiol. Stress 19, 100460. https://doi.org/10.1016/j.ynstr.2022.100460.
Perlman, G., Tanti, A., Mechawar, N., 2021. Parvalbumin interneuron alterations in stress-related mood disorders: A systematic review. Neurobiol. Stress 15, 100380. https://doi.org/10.1016/j.ynstr.2021.100380.
Qiu, S., Hu, Y., Huang, Yiming, Gao, T., Wang, Xiaofei, Wang, Danying, Ren, B., Shi, X., Chen, Y., Wang, Xinran, Wang, Dan, Han, L., Liang, Y., Liu, D., Liu, Q., Deng, L., Chen, Z., Zhan, L., Chen, T., Huang, Yuzhe, Wu, Q., Xie, T., Qian, L., Jin, C., Huang, J., Deng, W., Jiang, T., Li, X., Jia, X., Yuan, J., Li, A., Yan, J., Xu, N., Xu, L., Luo, Q., Poo, M.-M., Sun, Y., Li, C.T., Yao, H., Gong, H., Sun, Y.-G., Xu, C., 2024. Whole-brain spatial organization of hippocampal single-neuron projectomes. Sci. 383 eadj9198. https://doi.org/10.1126/science.adj9198.
Ribot, J., Breton, R., Calvo, C.-F., Moulard, J., Ezan, P., Zapata, J., Samama, K., Moreau, M., Bemelmans, A.-P., Sabatet, V., Dingli, F., Loew, D., Milleret, C., Billuart, P., Dallérac, G., Rouach, N., 2021. Astrocytes close the mouse critical period for visual plasticity. Science 373, 77–81. https://doi.org/10.1126/science.abf5273.
Romberg, C., Yang, S., Melani, R., Andrews, M.R., Horner, A.E., Spillantini, M.G., Bussey, T.J., Fawcett, J.W., Pizzorusso, T., Saksida, L.M., 2013. Depletion of Perineuronal Nets Enhances Recognition Memory and Long-Term Depression in the Perirhinal Cortex. J. Neurosci. 33, 7057–7065. https://doi.org/10.1523/JNEUROSCI.6267-11.2013.
Rossetti, A.C., Paladini, M.S., Colombo, M., Gruca, P., Lason-Tyburkiewicz, M., Tota-Glowczyk, K., Papp, M., Riva, M.A., Molteni, R., 2018. Chronic Stress Exposure Reduces Parvalbumin Expression in the Rat Hippocampus through an Imbalance of Redox Mechanisms: Restorative Effect of the Antipsychotic Lurasidone. Int. J. Neuropsychopharmacol. 21, 883–893. https://doi.org/10.1093/ijnp/pyy046.
Rymar, V.V., Sadikot, A.F., 2007. Laminar fate of cortical GABAergic interneurons is dependent on both birthdate and phenotype. J. Comp. Neurol. 501, 369–380. https://doi.org/10.1002/cne.21250.
Salaün, C., Courvalet, M., Rousseau, L., Cailleux, K., Breton, J., Bôle-Feysot, C., Guérin, C., Huré, M., Goichon, A., do Rego, J.-C., Déchelotte, P., Ribet, D., Achamrah, N., Coëffier, M., 2024. Sex-dependent circadian alterations of both central and peripheral clock genes expression and gut–microbiota composition during activity-based anorexia in mice. Biol. Sex. Differ. 15, 6. https://doi.org/10.1186/s13293-023-00576-x.
Schalla, M.A., Stengel, A., 2019. Activity Based Anorexia as an Animal Model for Anorexia Nervosa–A Systematic Review. Front. Nutr. 6.
Scharner, S., Stengel, A., 2019. Alterations of brain structure and functions in anorexia nervosa. Clin. Nutr. Exp. 28, 22–32. https://doi.org/10.1016/j.yclnex.2019.02.001.
Schindelin, J., Arganda-Carreras, I., Frise, E., Kaynig, V., Longair, M., Pietzsch, T., Preibisch, S., Rueden, C., Saalfeld, S., Schmid, B., Tinevez, J.-Y., White, D.J., Hartenstein, V., Eliceiri, K., Tomancak, P., Cardona, A., 2012. Fiji: an open-source platform for biological-image analysis. Nat. Methods 9, 676–682. https://doi.org/10.1038/nmeth.2019.
Selten, M., van Bokhoven, H., Nadif Kasri, N., 2018. Inhibitory control of the excitatory/inhibitory balance in psychiatric disorders. F1000Research 7, 23. https://doi.org/10.12688/f1000research.12155.1.
Shi, H.-J., Wang, S., Wang, X.-P., Zhang, R.-X., Zhu, L.-J., 2023. Hippocampus: Molecular, Cellular, and Circuit Features in Anxiety. Neurosci. Bull. 39, 1009–1026. https://doi.org/10.1007/s12264-023-01020-1.
Sigurdsson, T., Duvarci, S., 2015. Hippocampal-Prefrontal Interactions in Cognition, Behavior and Psychiatric Disease. Front. Syst. Neurosci. 9, 190. https://doi.org/10.3389/fnsys.2015.00190.
Slaker, M.L., Harkness, J.H., Sorg, B.A., 2016. A standardized and automated method of perineuronal net analysis using Wisteria floribunda agglutinin staining intensity. IBRO Rep. 1, 54–60. https://doi.org/10.1016/j.ibror.2016.10.001.
Suttkus, A., Rohn, S., Weigel, S., Glöckner, P., Arendt, T., Morawski, M., 2014. Aggrecan, link protein and tenascin-R are essential components of the perineuronal net to protect neurons against iron-induced oxidative stress. e1119 Cell Death Dis. 5, e1119. https://doi.org/10.1038/cddis.2014.25.
Tansley, S., Gu, N., Guzmán, A.U., Cai, W., Wong, C., Lister, K.C., Muñoz-Pino, E., Yousefpour, N., Roome, R.B., Heal, J., Wu, N., Castonguay, A., Lean, G., Muir, E.M., Kania, A., Prager-Khoutorsky, M., Zhang, J., Gkogkas, C.G., Fawcett, J.W., Diatchenko, L., Ribeiro-da-Silva, A., De Koninck, Y., Mogil, J.S., Khoutorsky, A., 2022. Microglia-mediated degradation of perineuronal nets promotes pain. Science 377, 80–86. https://doi.org/10.1126/science.abl6773.
Terstege, D.J., Goonetilleke, D., Barha, C.K., Epp, J.R., 2024. Running-induced neurogenesis reduces CA1 perineuronal net density without substantial temporal delay. Mol. Brain 17, 64. https://doi.org/10.1186/s13041-024-01138-x.
Tewari, B.P., Chaunsali, L., Prim, C.E., Sontheimer, H., 2022. A glial perspective on the extracellular matrix and perineuronal net remodeling in the central nervous system. Front. Cell. Neurosci. 16. https://doi.org/10.3389/fncel.2022.1022754.
Thompson, C.L., Pathak, S.D., Jeromin, A., Ng, L.L., MacPherson, C.R., Mortrud, M.T., Cusick, A., Riley, Z.L., Sunkin, S.M., Bernard, A., Puchalski, R.B., Gage, F.H., Jones, A.R., Bajic, V.B., Hawrylycz, M.J., Lein, E.S., 2008. Genomic Anatomy of the Hippocampus. Neuron 60, 1010–1021. https://doi.org/10.1016/j.neuron.2008.12.008.
Tose, K., Takamura, T., Isobe, M., Hirano, Y., Sato, Y., Kodama, N., Yoshihara, K., Maikusa, N., Moriguchi, Y., Noda, T., Mishima, R., Kawabata, M., Noma, S., Takakura, S., Gondo, M., Kakeda, S., Takahashi, M., Ide, S., Adachi, H., Hamatani, S., Kamashita, R., Sudo, Y., Matsumoto, K., Nakazato, M., Numata, N., Hamamoto, Y., Shoji, T., Muratsubaki, T., Sugiura, M., Murai, T., Fukudo, S., Sekiguchi, A., 2024. Systematic reduction of gray matter volume in anorexia nervosa, but relative enlargement with clinical symptoms in the prefrontal and posterior insular cortices: a multicenter neuroimaging study. Mol. Psychiatry 29, 891–901. https://doi.org/10.1038/s41380-023-02378-4.
Treccani, G., Musazzi, L., Perego, C., Milanese, M., Nava, N., Bonifacino, T., Lamanna, J., Malgaroli, A., Drago, F., Racagni, G., Nyengaard, J.R., Wegener, G., Bonanno, G., Popoli, M., 2014. Acute stress rapidly increases the readily releasable pool of glutamate vesicles in prefrontal and frontal cortex through non-genomic action of corticosterone, 401 Mol. Psychiatry 19, 401. https://doi.org/10.1038/mp.2014.20.
Ueno, H., Suemitsu, S., Murakami, S., Kitamura, N., Wani, K., Okamoto, M., Matsumoto, Y., Ishihara, T., 2017a. Region-specific impairments in parvalbumin interneurons in social isolation-reared mice. Neuroscience 359, 196–208. https://doi.org/10.1016/j.neuroscience.2017.07.016.
Ueno, H., Suemitsu, S., Murakami, S., Kitamura, N., Wani, K., Matsumoto, Y., Okamoto, M., Aoki, S., Ishihara, T., 2018. Juvenile stress induces behavioral change and affects perineuronal net formation in juvenile mice. BMC Neurosci. 19, 41. https://doi.org/10.1186/s12868-018-0442-z.
Ueno, H., Suemitsu, S., Okamoto, M., Matsumoto, Y., Ishihara, T., 2017b. Parvalbumin neurons and perineuronal nets in the mouse prefrontal cortex. Neuroscience 343, 115–127. https://doi.org/10.1016/j.neuroscience.2016.11.035.
Van De Werd, H.J.J.M., Rajkowska, G., Evers, P., Uylings, H.B.M., 2010. Cytoarchitectonic and chemoarchitectonic characterization of the prefrontal cortical areas in the mouse. Brain Struct. Funct. 214, 339. https://doi.org/10.1007/s00429-010-0247-z.
van Eeden, A.E., van Hoeken, D., Hoek, H.W., 2021. Incidence, prevalence and mortality of anorexia nervosa and bulimia nervosa. Curr. Opin. Psychiatry 34, 515–524. https://doi.org/10.1097/YCO.0000000000000739.
Wen, T.H., Binder, D.K., Ethell, I.M., Razak, K.A., 2018. The Perineuronal 'Safety' Net? Perineuronal Net Abnormalities in Neurological Disorders. Front. Mol. Neurosci. 11. https://doi.org/10.3389/fnmol.2018.00270.
Whittaker, R.G., Turnbull, D.M., Whittington, M.A., Cunningham, M.O., 2011. Impaired mitochondrial function abolishes gamma oscillations in the hippocampus through an effect on fast-spiking interneurons. Brain 134, e180. https://doi.org/10.1093/brain/awr018.
Yamada, J., Jinno, S., 2013. Spatio-temporal differences in perineuronal net expression in the mouse hippocampus, with reference to parvalbumin. Neuroscience 253, 368–379. https://doi.org/10.1016/j.neuroscience.2013.08.061.
Yamada, J., Ohgomori, T., Jinno, S., 2015. Perineuronal nets affect parvalbumin expression in GABAergic neurons of the mouse hippocampus. Eur. J. Neurosci. 41, 368–378. https://doi.org/10.1111/ejn.12792.